molecular pharmaceutics

ARTICLE

pubs.acs.org/molecularpharmaceutics

A Compound That Inhibits the HOP−Hsp90 Complex Formation and Has Unique Killing Effects in Breast Cancer Cell Lines

Genaro Pimienta, Kristina M. Herbert, and Lynne Regan*

Department of Molecular Biophysics and Biochemistry, Yale University, New Haven, Connecticut, United States

Supporting Information

ABSTRACT: The chaperone Hsp90 is required for the correct folding and maturation of certain "client proteins" within all cells. Hsp90-mediated folding is particularly important in cancer cells, because upregulated or mutant oncogenic proteins are often Hsp90 clients. Hsp90 inhibitors thus represent a route to anticancer agents that have the potential to be active against several different types of cancer. Currently, various Hsp90 inhibitors that bind to Hsp90 at its ATP-binding site are in preclinical and clinical trials. Some of the most promising Hsp90 ATP-binding site inhibitors are the well characterized geldanamycin derivative 17-AAG and the recently described compounds PU-H71 and NVP-AUY922. An undesirable characteristic of these compounds is the transcriptional upregulation of Hsp70 that has prosurvival effects. Here we characterize the activity of a new type of chaperone inhibitor, 1,6-dimethyl-3-propylpyrimido[5,4-*e*][1,2,4]triazine-5,7-dione (named C9 for simplicity). Using purified protein components *in vitro*, C9 prevents Hsp90 from interacting with the cochaperone HOP and is thus expected to impair the Hsp90-dependent folding pathway *in vivo*. We show that this compound is effective in killing various breast cancer cell lines including the highly metastatic MDA-MB-231. An important property of this compound is that it does not induce the transcriptional upregulation of Hsp70. Moreover, when cells are treated with a combination of C9 and either 17-AAG or NVP-AUY922, the overexpression of Hsp70 is counteracted considerably and C9's lethal-IC50 decreases compared to its value when added alone.

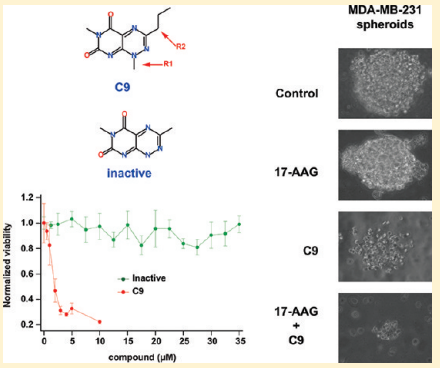

KEYWORDS: triple negative breast cancer, chaperone inhibitor, Hsp70, p38, JNK1/2

INTRODUCTION

The chaperone Hsp90 is a well-established anticancer drug target.[1,2] Hsp90 is responsible for the folding of numerous proteins into their mature, functional state.[3] Many such Hsp90 "client proteins" are involved in key oncogenic pathways including proliferation, cell cycle progression, inhibition of apoptosis and metastasis.[4,5] When Hsp90 is inhibited, Hsp90-dependent client proteins are ubiquitinated and thus targeted for proteasomal degradation.[6−9] Inhibitors of Hsp90 therefore have the potential to be effective against a broad range of different cancer types.[7]

The natural product geldanamycin and its derivatives such as 17-AAG inhibit Hsp90 by binding to its N-terminal domain at the ATP-binding site.[10,11] Treatment of cells with such compounds indeed results in the degradation of a large number of client proteins that are involved in oncogenic pathways.[12−15] The mechanism of action of 17-AAG has been well studied.[1,2] Recently however, various other Hsp90 ATP-binding site inhibitors, such as PU-H71 and NVP-AUY922, have been described and are together with 17-AAG in clinical trials.[1,2] A component of resistance common to these Hsp90 ATP-binding site inhibitors is thought to be the transcriptional induction of a heat shock response: overproduction of Hsp27 and Hsp70, which have strong antiapoptotic activity.[16−19]

We have recently described a new class of chaperone inhibitors that prevent the interaction of Hsp90 with the protein HOP (Hsp70-Hsp90 organizing protein) *in vitro*.[20] In the folding pathway of Hsp90 client proteins, folding is initiated on Hsp70, and the partially folded protein is then transferred to Hsp90, where the final stages of maturation are completed (Figure 1).[21] These reactions occur on the Hsp70−HOP−Hsp90 complex.[4,5] If Hsp90 is prevented from interacting with HOP, this complex can no longer form (Figure 1).[4,5] Here we investigate how one of these compounds (1,6-dimethyl-3-propylpyrimido[5,4-*e*][1,2,4]triazine-5,7-dione), which for simplicity we refer to as C9 (Supplementary Figure 1a in the Supporting Information), kills the highly metastatic triple negative breast cancer (TNBC) cell line MDA-MB-231. We have also extended the investigation of the most significant findings in other cancer cell lines.

We found that C9 induces a change in cell morphology and causes cell cycle arrest of MDA-MB-231 cells, with a consequent inhibition of spheroid formation and cell migration. The killing activity of C9 against MDA-MB-231 cells is not via a pathway that involves the activation of the apoptosis mediators Caspase 3/7. This result is unique because the currently available Hsp90

Received: March 13, 2011
Accepted: September 1, 2011
Revised: August 28, 2011
Published: September 01, 2011

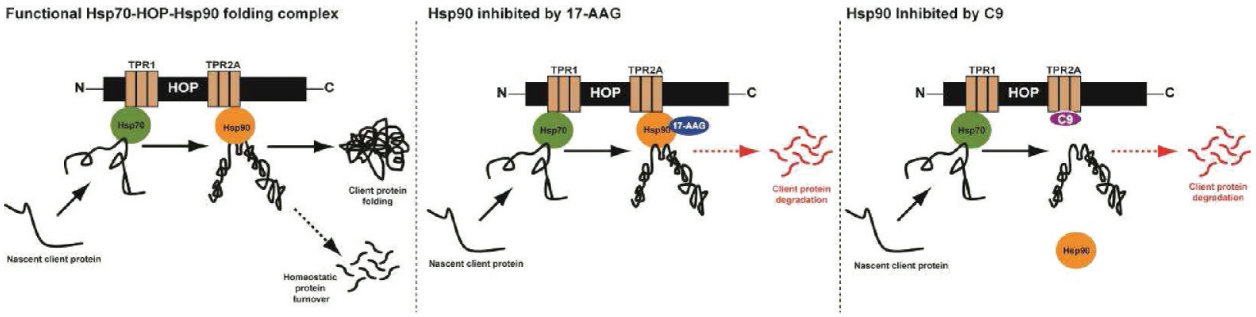

Figure 1. C9 and 17-AAG inhibit Hsp90 through different mechanisms. Cartoon representation of the Hsp90-mediated folding pathway and the points at which 17-AAG and C9 act to inhibit it. 17-AAG binds directly to Hsp90, at the ATP binding site of the N-terminal domain (middle). C9 binds to the TPR2A domain of HOP, thus preventing the C-terminus of Hsp90 from binding to HOP (right).

ATP-binding site inhibitors, such as 17-AAG, PU-H71 and NVP-AUY922, induce Caspase 3/7-mediated apoptotic cell death.[18,22]

At the molecular level C9 like 17-AAG induces the degradation of the well-established Hsp90 client proteins CDK4 and Raf-1. An unexpected yet interesting result is the C9-mediated protein downregulation of the mitogen activated protein kinases (MAPKs) JNK1/2 and p38, also known as stress-activated protein kinases (SAPKs), for which a dependency on the Hsp90 folding pathway is not yet fully established.[23−27] The decrease in the protein levels of these kinases is significant, because when overactive they are known to drive the tumorigenic phenotype in malignant cell lines.

Remarkably, treatment of cells with C9 does not result in the undesirable increase in the protein levels of Hsp27 and Hsp70, which is characteristic of the aforementioned ATP-binding site Hsp90 inhibitors. Furthermore, when cells are treated with a combination of C9 and either 17-AAG or NVP-AUY922, the effect of C9 is dominant and the upregulation of Hsp27 and Hsp70 is suppressed considerably.

MATERIALS AND METHODS

Cell Culture. All cell lines were cultured in high glucose Dulbecco's modified Eagle's medium (DMEM) supplemented with L-glutamine and sodium pyruvate (Invitrogen), plus 10% v/v fetal bovine serum (FBS) heat inactivated (Gibco), 1% v/v of penicillin/streptomycin 10,000 units (Gibco) and 10 μM of recombinant insulin (Sigma). Cells were grown to about 80% confluency, and then synchronized by serum starvation for 24 h prior to adding inhibitory compounds.

Caspase 3/7 Activity and Viability Assays. Intracellular Caspase 3/7 activity and cell viability in the form of metabolic ATP content were quantified using the CellTiter Caspase 3/7 (Promega) or the CellTiter-Glow (Promega) luminescent assays, respectively. In both assays, cells were seeded in 96-well opaque plates (Corning), serum starved for about 24 h so that most of the cells were synchronized in a resting population, and then treated with 10% FBS and insulin, plus either C9, 17-AAG, PU-H71, NVP-AUY922 or H_2O_2, typically for 24 h.

For these and all experiments (unless noted otherwise) the concentration of C9 was 3 μM and the concentration of 17-AAG, PU-H71, and NVP-AUY922 was 1 μM.

After 24 h of drug treatment, the tissue culture plates were treated with either CellTiter Caspase 3/7 (Promega) or CellTiter-Glo (Promega) reagent following the manufacturer's protocol. Caspase 3/7 activity and viability (metabolic ATP content) as a function of relative fluorescent intensity were measured on an ENVISION plate reader using a luminescence filter.

Poly-HEMA Coating of Plates To Prevent Cell Attachment. 6-Well plates were treated with 1 mL/per well of 0.5% w/v of Poly-HEMA (Sigma) dissolved in 95% ethanol. This solution was left overnight to dry completely in a sterile cell culture hood, and the procedure was repeated 5 more times, to ensure a homogeneous coating of the plate surface. Before use, the plate was washed twice with sterile phosphate buffered saline (PBS) solution (Gibco) to remove any traces of chemical contaminants.

3D-Spheroid Generation. Matrigel was used to assist the spheroid formation of MDA-MB-231cells. A cell suspension in DMEM growth medium, with 2.5% v/v cold Matrigel matrix (BD Biosciences), was added to a plate previously treated with poly-HEMA and allowed to grow nonattached. In the case of MCF7 and BT-474 cells, the addition of Matrigel was not necessary, because unlike MDA-MB-231 cells, these two cell lines form spontaneous 3D spheroids even in the absence of Matrigel.

Microscope Cell Imaging. Cell images were obtained by phase contrast with an inverted microscope (Olympus CKX41), at 20−40× magnification. Pictures were taken with a digital camera interfaced to a PC desktop computer. Each image was cropped and its brightness/contrast adjusted in ImageJ.

Wound-Healing/Scratch Assay. Cells were grown to about 80% confluency and then synchronized by serum starvation for 24 h. A sterile 200 μL pipet tip was used to scratch across the plate, making a "wound" in the cell layer. The medium was then removed by aspiration and the cellular monolayer washed 5 times with serum free medium to remove the detached cells from the scratch. FBS-containing DMEM medium plus either DMSO (control), C9 or 17-AAG was added to each plate, and the samples were left to grow. The width of the scratch was documented by photographing the cells as described above every 12 h.

FACS Cell Cycle Analysis. For DNA-cell cycle analysis, confluent cells from a 10 cm plate were detached with trypsin-EDTA, washed with cold PBS and harvested in FACS polypropylene tubes. Cell pellets were resuspended in prechilled 70% ethanol and incubated at 4 °C for at least an hour to allow DNA fixing. Next, the samples were washed 3 times with cold PBS and treated with 100 μL of DNase free ribonuclease 100 μg/mL (Sigma) for 10 min at room temperature. This was followed by the addition of 400 μL of propidium iodide dissolved in PBS at 50 μg/mL and protected from light. Stained samples were analyzed on a FACScan instrument at the Yale University School of Medicine Cell Sorter Facility.

Western Blots (WB). Cells were harvested by centrifugation and lysed with a solution containing 50 mM Tris-Base (pH 7.6), 150 mM NaCl, 1.5 mM EDTA, 1% v/v Nonidet-P40 and 10% v/v glycerol. To inhibit proteases and phosphatases, 50 mL of cold lysis solution was freshly mixed with a tablet of a cocktail of protease inhibitors (Sigma) and 100 μL of phosphatase inhibitor cocktails I and II (Sigma).

Total protein concentration in each extract was determined using the Bradford protein assay (Bio-Rad). Based on these concentrations, equal amounts of total protein from each extract were separated by SDS polyacrylamide gel electrophoresis, followed by the electrotransfer of proteins onto a nitrocellulose membrane. The transferred blot was blocked with either 5% fat-free milk or 5% bovine serum albumin in a Tween20/Tris-Base saline solution (TTBS), at 4 °C overnight and probed with specific antibodies purchased from Cell Signaling Technology, also at 4 °C overnight. The blots were then washed with TTBS and incubated with a species-specific IgG secondary antibody coupled to horseradish peroxidase (HRP), for an hour at room temperature. To detect the HRP signal, an acridan-based reagent (ECL-Plus from Amersham) was added to each blot followed by autoradiography on a film.

qRT-PCR. RNA was isolated using TRIzol (Invitrogen), DNase treated (RNase-Free DNase Set, Qiagen), and then purified on RNeasy Mini cleanup columns (Qiagen). The High Capacity cDNA Reverse Transcription Kit (Applied Biosystems) was used according to the manufacturer's protocol. The qRT-PCR experiments were performed using the 7900HT Fast Real-Time PCR System using Taqman assays (Applied Biosystems) for the individual genes. Taqman assay IDs were as follows: RPL30 control (Hs00265497_m1), Hsp27 (Hs00356629_g1) and Hsp70 (Hs00271229_s1). RPL30 was determined to be an appropriate normalization control in an initial experiment in which isolated cDNA was run on a TaqMan Array Gene Signature 96-well human endogenous control plate. Of the 32 control genes present on this plate, RPL30 showed the least variability in amplification cycle number between cells treated with DMSO, C9, or 17AAG. The mRNA levels of each gene were normalized to the value obtained for the RPL30 mRNA transcript in the same sample. The normalized values obtained from MDA-MB-231 cells treated with C9 or 17-AAG, were normal ized once more with respect to values obtained in the DMSO-treated sample.

RESULTS

We have previously described compounds with a common pyrimidotriazinedione structural core that inhibit the Hsp90-dependent folding pathway by a novel mechanism. *In vitro*, these compounds inhibit the interaction of the TPR2A domain of HOP with the C-terminus segment of Hsp90, and are thus expected to impair the formation of a functional Hsp70−HOP−Hsp90 complex *in vivo*.[20,28] Here we present a characterization of the effects of one of these compounds, C9 (1,6-dimethyl-3-propylpyrimido[5,4-*e*][1,2,4]triazine-5,7-dione) (Supplementary Figure 1a in the Supporting Information), on the highly metastatic TNBC cell line MDA-MB-231. The TNBC subtype does not express detectable levels of estrogen and progesterone receptors (ER and PR, respectively) or the human epidermal growth factor receptor 2 (HER2).[29]

Furthermore, MDA-MB-231 cells have been reported to be relatively insensitive to 17-AAG.[30] So far, PU-H71 and NVP-AUY922 are the only Hsp90 ATP-binding site inhibitors that kill MDA-MB-231 cells.[18,22] However, the killing effects of PU-H71 and NVP-AUY922 against MDA-MB-231 cells can only be observed at 72 h.[18,22]

Using 24 h treatments, we compare and contrast the effects of C9 with those of 17-AAG, which is an Hsp90 inhibitor with a well established mechanism of action. Furthermore, because 17-AAG and C9 are proposed to inhibit Hsp90 by completely different mechanisms (Figure 1), we also investigate the effects of treating cells with a combination of both compounds. To better demonstrate the most important features of C9, we also show comparisons with PU-H71 and NVP-AUY922, which, like 17-AAG, are ATP-binding site inhibitors of Hsp90 that induce an increase in the mRNA and protein levels of Hsp70.

Specificity of Action: *In Vivo* Activity of C9 vs a Derivative That Does Not Inhibit the HOP−Hsp90 Interaction *in Vitro*. In our initial studies we tested compounds with a common 7-azapteridine ring system (pyrimido[5,4-*e*][1,2,4]triazine-5,7-dione).[20,28] One of these compounds is unsubstituted at position 1, and is inactive in the *in vitro* assays for inhibition of the Hsp90−HOP interaction[20] (Figure 2a). To determine the specificity of C9 in killing TNBC cell lines, we performed cell viability assays as a function of compound concentration in MDA-MB-231 cells treated with either C9 or the inactive compound (Figure 2b). C9, which is the compound that inhibits the interaction of Hsp90 with HOP *in vitro*, kills MDA-MB-231 cells with a lethal-IC50 of about 2 μM (Figure 2b). The inactive compound that does not inhibit the HOP−Hsp90 interaction *in vitro* fails to kill MDA-MB-231 cells, even at a 35 μM final concentration (Figure 2b). C9 is also effective at killing another TNBC cell line, MDA-MB-468 at an approximate lethal-IC50 of about 1.75 μM (Supplementary Figure 1b in the Supporting Information).

Taken together, these results strongly support the conclusion that the predominant cause of C9's cellular effects against TNBC cell lines reported in this paper is its ability to inhibit the Hsp90−HOP interaction.

C9 Has a Lower Lethal-IC50 When Added in Combination with Hsp90 Inhibitors. We next investigated the cell killing activity of 17-AAG, PU-H71 and NVP-AUY922 and found as reported previously[18,22,30] that in a 24 h treatment MDA-MB-231 cells are relatively insensitive to these compounds (Figure 2c). Treating MDA-MB-231 cells for up to 96 h with C9 (3 μM) or 17-AAG (1 μM) shows that 17-AAG was relatively ineffective even out to 96 h, while C9 exerts its effects quickly within the first 24 h (Supplementary Figure 1c in the Supporting Information).

Despite their inability to kill MDA-MB-231 cells in a 24 h treatment, these compounds are still expected to interact with Hsp90 inside cells and inhibit its ATPase activity. We therefore tested whether these compounds, by inhibiting the chaperone pathway by an alternate mechanism, may decrease the lethal-IC50 of C9. To do this we added a constant amount of either 17-AAG, PU-H71 or NVP-AUY922 (1 μM) to increasing concentrations of C9. We found that in comparison to C9 alone (lethal-IC50 about 2 μM), the lethal-IC50 of C9 against MDA-MB-231 is lower when combined with a constant 1 μM of either 17-AAG (lethal-IC50 about 0.50 μM) or NVP-AUY922 (lethal-IC50 about 1 μM), but not with PU-H71 (lethal-IC50 about 2 μM), (Figure 2d). Taken with caution, these results show that despite their inefficacy against MDA-MB-231 in a 24 h treatment at least two of the Hsp90 inhibitors tested (17-AAG and

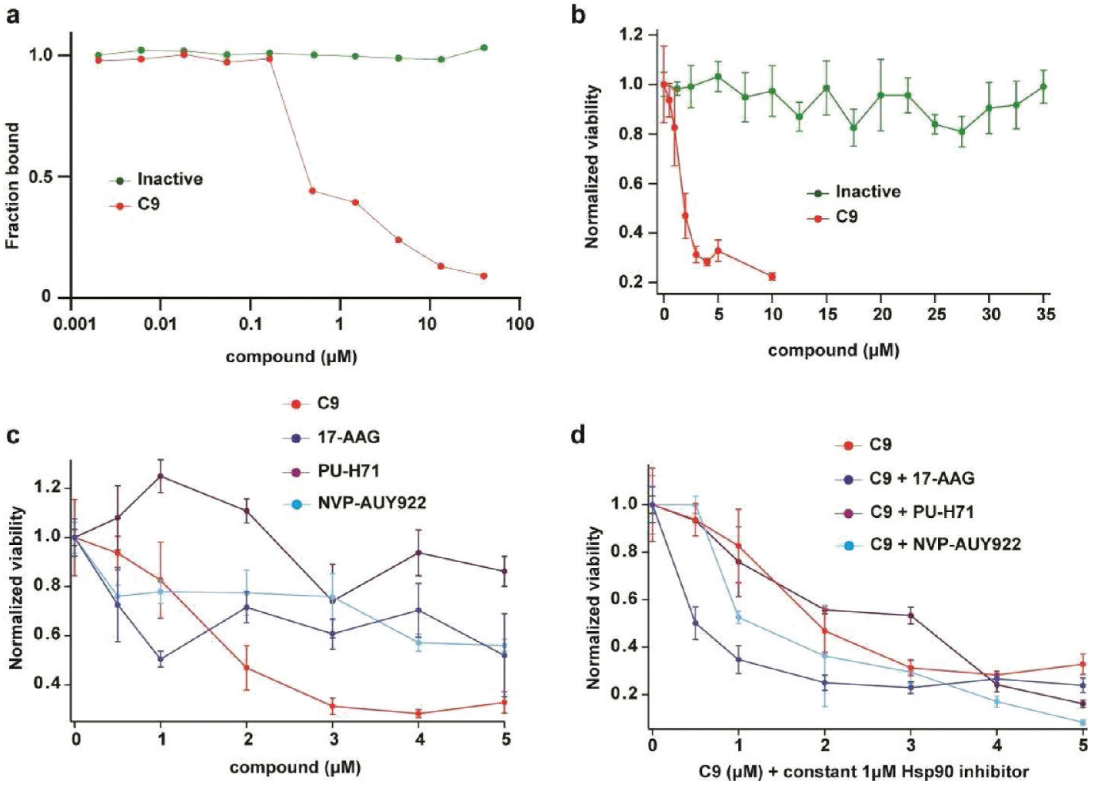

Figure 2. *In vitro* and *in vivo* activity of C9. (a) Plot showing inhibition of the interaction of TPR2A (the Hsp90-binding domain of HOP) with the C-terminal peptide of Hsp90 in an *in vitro* AlphaScreen assay.[16,24] Fraction bound is plotted versus the concentration of either C9 or the inactive derivative. Adapted from ref 16. (b) Dose−response killing assays of MDA-MB-231 cells cultured as adherent monolayers when treated 24 h with C9 (0−10 μM) or the inactive compound (0−35 μM). (c) Dose−response killing assays of MDA-MB-231 cells cultured as adherent monolayers when treated 24 h with C9, 17-AAG, PU-H71 or NVP-AUY922. (d) Dose−response killing assays of MDA-MB-231 cells cultured as adherent monolayers when treated 24 h with C9 or combination of C9 plus a constant amount (1 μM) of either 17-AAG, PU-H71 or NVP-AUY922. In the dose−response killing assays, each data point is the average of 6 biological replicates normalized to the average viability measured in cells treated with DMSO. Cell viability was determined by measuring cellular ATP content using the CellTiter-Glow (Promega) luminescent assay.

NVP-AUY922) potentiate the killing effects of C9, by reducing its lethal-IC50. Finally, while this data highlights the potential of C9 in combination therapies aimed at disrupting the Hsp90 folding pathway in cancer cells, further experimentation is required to truly establish quantitatively a synergistic effect between C9 and either 17-AAG or NVP-AUY922.

C9, but Not 17-AAG, Inhibits MDA-MB-231 Spheroid Formation. We next investigated the effects of C9, 17-AAG, and a combination of the two compounds on MDA-MB-231 cells grown as nonadherent 3-dimensional (3D) spheroids. C9 treatment inhibits spheroid formation and kills MDA-MB-231 cells cultured in the 3D spheroid form, whereas 17-AAG has little or no effect (Figure 3a). When MDA-MB-231 spheroids are treated with a combination of C9 and 17-AAG, the effect of C9 is dominant. That is, spheroid formation is inhibited and cells are killed (Figure 3a). The observation that C9 kills MDA-MB-231 cells when cultured as 3D-spheroids alone or in combination with 17-AAG is important, because the culture of breast cancer cell lines as nonattached aggregates in the presence of Matrigel extract is a better mimic of the tissue environment *in vivo*.[31,32]

C9 Destroys the Spheroids Formed by BT-474 and MCF7 Cells. We further corroborated the ability of C9 to kill breast cancer cell lines cultured as spheroids by testing two additional breast cancer cell lines, BT-474 and MCF7, both of which form 3D-spheroids even in the absence of Matrigel.[33,34] We showed in our previous work that C9 is effective at killing these non-TNBC cell lines when cultured as monolayers.[20] BT-474 cells belong to the HER2-positive breast cancer subtype and MCF7 cells are ER-positive.[29] We found that C9 disrupts spheroid formation and kills both of these two cell lines effectively (Figure 3b,c). 17-AAG is also effective in disruption and killing of these cell lines (Figure 3b,c). These results show that C9 on the one hand is effective in killing spheroids of different breast cancer subtypes, while 17-AAG on the other hand is ineffective against the TNBC MDA-MB-231 cells, but can kill the non-TNBC cell lines BT-474 and MCF7.

C9, but Not 17-AAG, Induces Cell-Shape Changes and Decreases Cell Migration. MDA-MB-231 cells have a spindle-like shape, have a mesenchymal phenotype, and are highly invasive.[35] Treatment of MDA-MB-231 cells with C9 causes them to acquire a cobblestone-like morphology, whereas treatment with 17-AAG does not (Figure 4a). This result suggests that C9 may decrease the migration properties of MDA-MB-231 cells. To follow up on this observation, we investigated the effects of C9 and 17-AAG in a "wound healing" scratch assay, as a proxy for metastatic potential. C9 impaired the migration properties of MDA-MB-231 cells, while 17-AAG did not (Figure 4b). The change in cell shape and the inhibition of migration *in vitro* are important observations because they suggest that C9 may be

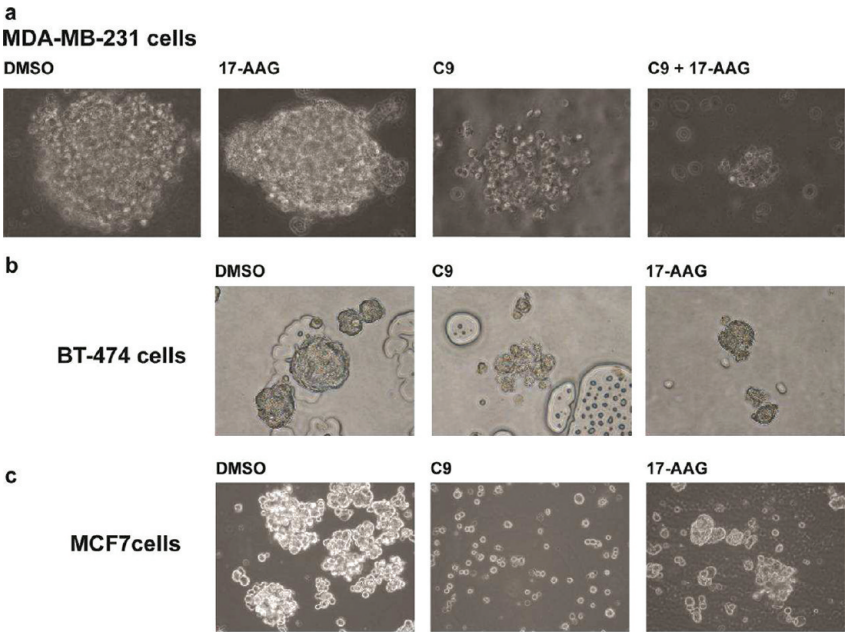

Figure 3. Effects of C9 and 17-AAG in breast cancer cell lines cultured as 3D spheroids. (a) Matrigel-assisted 3D spheroid formation of MDA-MB-231 cells on poly-HEMA coated plates, documented at 20× magnification (b) Spontaneous 3D spheroid formation of BT-474 cells on poly-HEMA coated plates, documented at 20× magnification. (c) Spontaneous 3D spheroid formation of MCF7 cells on poly-HEMA coated plates, documented at 20× magnification. In all cases, cell were treated 24 h with either C9 (3 μM), 17-AAG (1 μM) or a combination of C9 (3 μM) plus 17-AAG (1 μM).

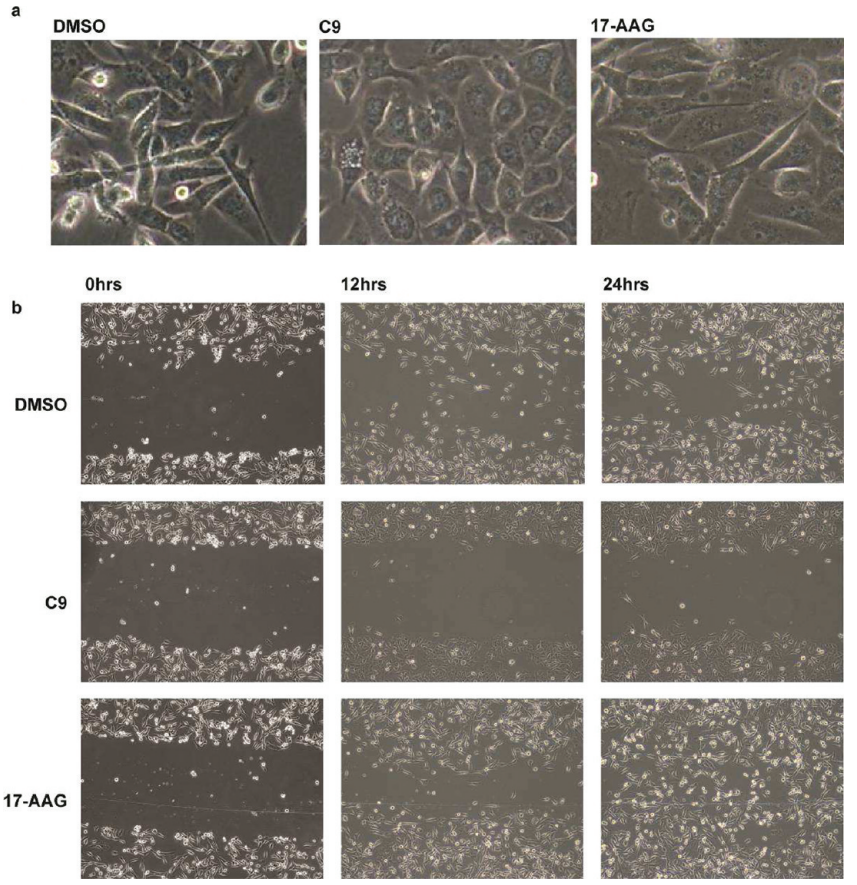

Figure 4. Effects C9 and 17-AAG on the cell shape and *in vitro* migration of MDA-MB-231 cells. (a) Cell shape of MDA-MB-231 cells observed at 40× magnification when treated 24 h with DMSO, C9 (3 μM) or 17-AAG (1 μM). (b) Wound-healing/scratch assay documented at 20× magnification after 0, 12, and 24 h of drug treatment. MDA-MB-231 cells were treated with DMSO, C9 (3 μM) or 17-AAG (1 μM).

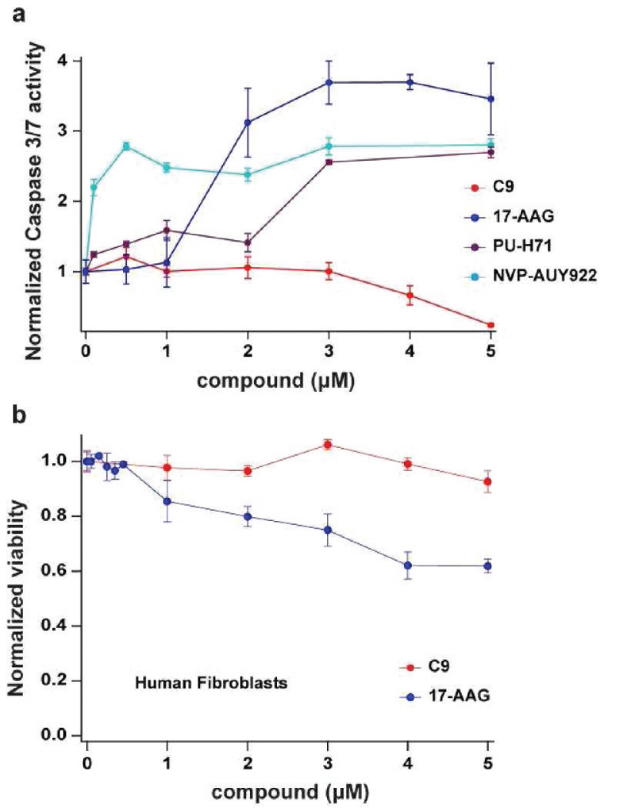

Figure 5. Cancer cell killing mode of C9. (a) Dose−response Caspase 3/7 activation assays of MDA-MB-231 cells cultured as adherent monolayers when treated 24 h with C9, 17-AAG, PU-H71 or NVP-AUY922. (b) Dose−response killing assays of human fibroblast cells cultured as adherent monolayers when treated 24 h with C9 or 17-AAG.

reversing the metastatic potential of this cell line, which is clearly a desirable characteristic.

Both C9 and 17-AAG Inhibit Cell Cycle Progression. The currently available Hsp90 ATP-binding site inhibitors such as 17-AAG commonly induce cell cycle arrest.[1,2] We therefore determined the effect of C9 and 17-AAG on the progression through the cell cycle, by monitoring the cellular DNA content using FACS. Serum depletion of MDA-MB-231 cells for 24 h arrests about 70% of cells in G1 (Supplementary Figure 2 in the Supporting Information). Addition of serum allows cells to progress through the cell cycle as seen in the DMSO-treated control sample where only about 45% of cells are in G1. Treatment of cells with either C9 or 17-AAG following serum starvation however prevents cell cycle progression and results in about 60% of cells in G1 (Supplementary Figure 2 in the Supporting Information). The ability of C9 to arrest cell cycle progression is a desirable property of an anticancer compound.

C9 Induces Cell Death without Activating the Apoptosis Mediators Caspase 3/7. To obtain mechanistic details about how C9 kills breast cancer cells, we investigated the ability of C9 to induce apoptosis via Caspase 3/7 activation, which is a typical effect of 17-AAG and other Hsp90 ATP-binding site inhibitors.[1,2] We found that even at a 5 μM final concentration C9 did not activate Caspase 3/7 (Figure 5a). The three Hsp90 ATP-binding site inhibitors tested (17-AAG, PU-H71 and NVP-AUY922) induced Caspase 3/7 activity (Figure 5a), to levels similar to those reported previously.[18,22] These results indicate that C9 not only inhibits the Hsp90-dependent folding pathway in a manner different from the ATP-binding site Hsp90 inhibitors like 17-AAG (Figure 1) but also induces a different mechanism of cell death. To further support this result, we corroborated the absence of Caspase 3/7 activation in C9-treated MDA-MB-231 cells with the PARP-cleavage assay (Supplementary Figure 3a in the Supporting Information).

Effects of C9 and 17-AAG on Nontumorigenic Cells in Culture (Human Fibroblasts). In the absence of Caspase 3/7 activation, an undesirable property of C9 would be that its killing effects are conducive to massive toxicity like in the case of unspecific anticancer drugs used in chemotherapy. To obtain an *in vitro* estimation of the toxicity of C9 in nontumorigenic cells, we compared the killing effects of C9 and 17-AAG on human fibroblasts cultured *in vitro*, as a surrogate for nontumorigenic tissue. We found that neither C9 nor 17-AAG kill human fibroblasts considerably even when added at a final concentration of 5 μM (Figure 5b). While it is premature to claim that C9 is universally not toxic to nontumorigenic cells, these results suggest great promise for C9 in future *in vivo* investigations.

Changes in the Levels of Hsp90 "Client" Proteins as a Consequence of C9 or 17-AAG Treatment. We investigated the effect of treating cells with C9, 17-AAG or a combination of the two compounds on the levels of the kinases AKT, CDK4, EGFR and Raf-1, which are well-documented Hsp90-dependent "client" proteins expressed at detectable levels in MDA-MB-231 cells. We also investigated the effects of C9 and 17-AAG on the levels of the mitogen activated protein kinases (MAPK) - ERK1/2, JNK1/2 and p38, for which the role of Hsp70 and Hsp90 has been suggested but is not yet fully established.[23−27] Finally, we used BT-474 cells to investigate the effects of C9 on the estrogen receptor (ER), which is a steroid receptor and a well characterized 17-AAG target.

Neither C9 nor 17-AAG nor a combination of the two compounds has an effect on AKT (Figure 6a). By contrast both C9 and 17-AAG cause a clear decrease in CDK4 levels, and a less drastic diminution in the case of EGFR and Raf-1 (Figure 6a). A combination of C9 and 17-AAG induced a more pronounced decrease in CDK4, EGFR and Raf-1 levels than either compound alone (Figure 6a).

ERK1/2 was not affected by C9, 17-AAG or a combination of the two compounds. In contrast, C9 and less dramatically 17-AAG decreased JNK1/2, and only C9 had a clear effect on the levels of p38 (Figure 6a).

The inability of 17-AAG to affect the protein stability of ERK1/2 has been extensively documented.[7] Additionally, it has been reported that the inhibition of Hsp90 by 17-AAG causes a decrease in HER2 levels more effectively than it induces a decrease in the levels of EGFR/HER1.[36] Also, the degree of AKT downregulation by Hsp90 inhibitors has been reported to vary in different cell lines.[37]

In the case of the ER we found that 17-AAG decreased the protein levels of this steroid receptor, while C9 did not affect this protein (Supplementary Figure 3b in the Supporting Information), further suggesting that in agreement with their different proposed mechanism of action (Figure 1), C9 and 17-AAG affect a different subset of Hsp90 client proteins (Figure 6a).

An Unexpected Effect of C9 Treatment Is the Decrease of the Protein Cdc37. In order to determine a possible mechanism for the unexpected decrease of the two structurally related SAPKs tested here (JNK1/2 and p38), we next investigated the protein levels of Cdc37, which is a cochaperone implicated in the regulation of Hsp90 client proteins with kinase activity.

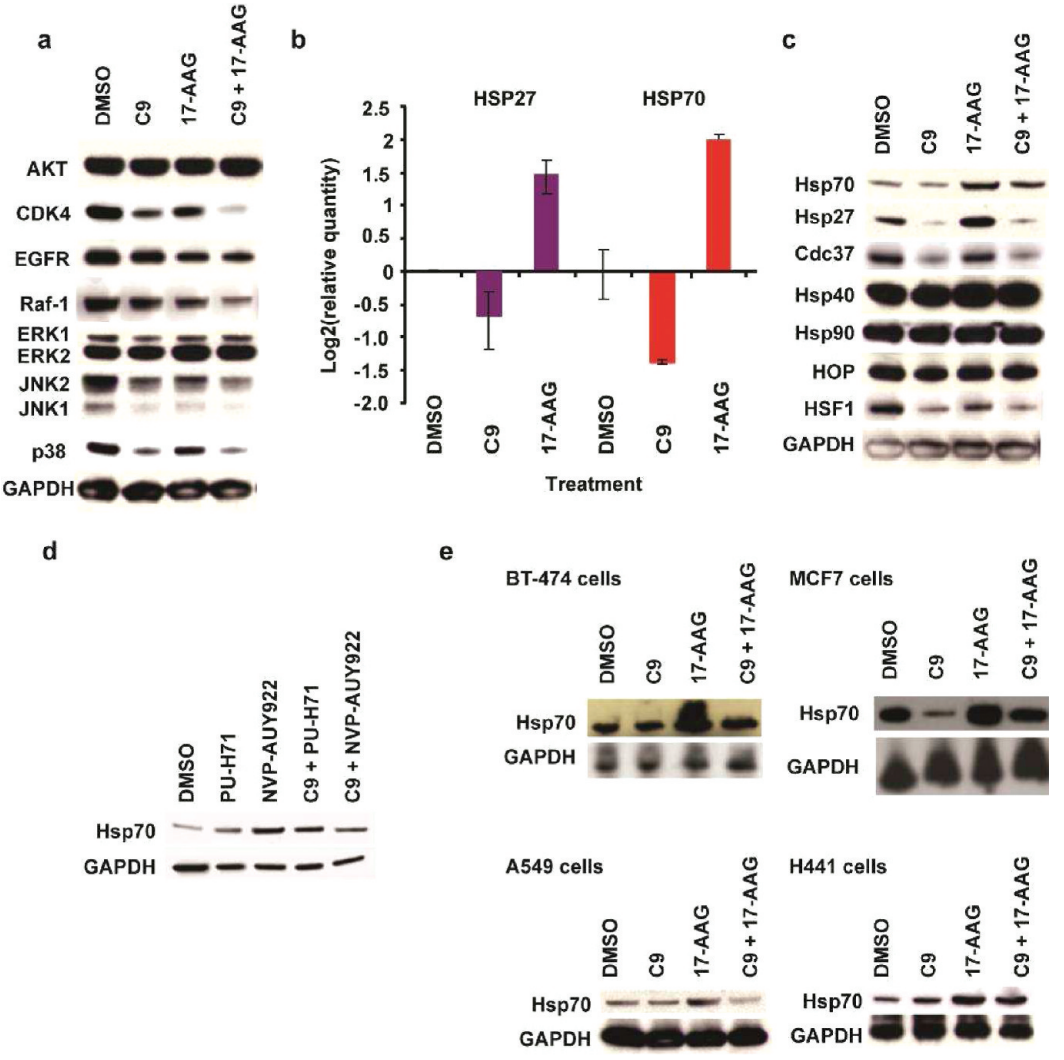

Figure 6. Effects of C9 and 17-AAG on the stability of Hsp90 client proteins and on the mRNA and protein levels of chaperones. (a) WB assays testing AKT, CDK4, EGFR, Raf-1, ERK1/2, JNK1/2 and p38 in MDA-MB-231 cells treated 24 h with DMSO, C9 (3 μM), 17-AAG (1 μM) or a combination of C9 (3 μM) plus 17-AAG (1 μM). (b) Normalized mRNA levels of the genes coding for Hsp27 and Hsp70 in MDA-MB-231 cells treated 24 h with DMSO, C9 (3 μM) or 17-AAG (1 μM). The mRNA values obtained by qRT-PCR were as follows: Hsp27 (DMSO = 1 $\pm$ 0.25, C9 = 0.63 $\pm$ 0.19, 17AAG = 2.7 $\pm$ 0.48); and Hsp70 (DMSO = 1, C9 = 0.38 $\pm$ 0.01, 17AAG = 3.9 $\pm$ 0.27). (c) WB assays testing Hsp70, Hsp27, Cdc37, Hsp40, Hsp90, HOP and HSF1 in MDA-MB-231 cells treated 24 h with DMSO, C9 (3 μM), 17-AAG (1 μM) or a mixture of C9 (3 μM) plus 17-AAG (1 μM). (d) WB assays testing Hsp70 in MDA-MB-231 cells treated 24 h with either PU-H71 (1 μM) or NVP-AUY922 (1 μM) alone, or with a combination of C9 (3 μM) plus either PU-H71 (1 μM) or NVP-AUY922 (1 μM). (e) WB assays testing Hsp70 in two breast cancer cell lines (BT-474 and MCF7) and two lung cancer cell lines (A549 and H441), treated 24 h with DMSO-control, C9 (3 μM), 17-AAG (1 μM) or a combination of C9 (3 μM) plus 17-AAG (1 μM).

The kinase-specific cochaperone Cdc37 is encoded by an inducible gene found overexpressed in various cancer types, and is thus considered a drug target.[5] Both Cdc37 knockdown and Celastrol, a compound that inhibits the Hsp90−Cdc37 heterocomplex, reduce the protein levels of the Hsp90 clients.[38,39] Additionally, it has recently been shown that Cdc37 regulates the activity of p38.[40] Our results show that, unlike 17-AAG, C9 alone or combined with 17-AAG reduces the protein levels of Cdc37 considerably (Figure 6c).

This result shows that C9 has unexpected effects on at least one of the cochaperones associated with the Hsp70−HOP−Hsp90 heterocomplex and may underpin the C9-mediated decrease in the protein levels of p38 and JNK1/2.

Changes in Chaperone Levels Induced by C9 and 17-AAG. 17-AAG and other Hsp90 ATP-binding site inhibitors typically induce an increase in the mRNA and protein levels of the chaperones Hsp27 and Hsp70.[16−19] We therefore monitored changes in the mRNA and protein levels of Hsp27 and Hsp70 following treatment of MDA-MB-231 cells with C9 or 17-AAG. Treatment of MDA-MB-231 cells with C9 results in a decrease in the mRNA levels of Hsp27 and Hsp70. By contrast, treatment of these cells with 17-AAG induced an increase in the mRNA levels of Hsp27 and Hsp70 (Figure 6b). The changes in mRNA levels were accompanied by corresponding increases or decreases in protein levels (Figure 6c). As a control for nonspecific protein degradation due to C9-mediated cell death, we determined the protein levels of Hsp90 and the cochaperones Hsp40 and HOP, and observed no changes (Figure 6c).

It is well documented that treatment of cells with Hsp90 ATP-binding site inhibitors, such as 17-AAG, PU-H71 and

NVP-AUY922, causes an increase in the cellular levels of Hsp70.[16−19] This side effect is undesirable, because Hsp70 has antiapoptotic properties.[41] We therefore investigated the effect of combining 17-AAG treatment, which causes an increase in Hsp70 levels, with C9 treatment, which causes a decrease in Hsp70 levels. We observed that in MDA-MB-231 cells treated with C9 plus 17-AAG the overexpression of Hsp70 is dampened, compared to the levels induced by 17-AAG (Figure 6c). C9 had a similar effect on Hsp70 when combined with NVP-AUY922, but not with PU-H71 (Figure 6d). Interestingly, these results correlate with the finding that a combination of C9 plus 17-AAG or NVP-AUY922, but not PU-H71, decreases C9's lethal-IC50 (Figure 2d).

To better demonstrate the effects of C9 when combined with an Hsp90 ATP-binding site inhibitor such as 17-AAG, we next determined Hsp70's protein levels in various other cell lines, besides MDA-MB-231. While the decrease in the levels of Hsp70 induced by C9 varied between cell lines, a combination of C9 with 17-AAG prevented the upregulation of Hsp70, normally induced by 17AAG alone, in all cases (Figure 6e).

The ability of C9 to counterbalance the upregulation of Hsp70 induced by Hsp90 ATP-binding site inhibitors is an important result because it suggests that an added advantage to a combination of C9 and either 17-AAG or NVP-AUY92 in cancer therapy would be to antagonize their prosurvival side effects, by counteracting the increase in Hsp70 levels induced by these compounds when added alone.

Furthermore, while a 3 μM C9 final concentration is lethal against the breast cancer cell lines BT-474 and MCF7 (Figures 3b and 3c), this dose does not have an obvious killing effect against the two lung cancer cell lines A549 and H441 as shown by pictures taken of these cells after C9 treatment (Supplementary Figure 4 in the Supporting Information). Considering that the combination of two anticancer drugs may enhance toxicity, our results highlight the potential use of C9 at sublethal doses in combination with Hsp90 inhibitors like 17-AAG or NVP-AUY922 to suppress the transcriptional upregulation of Hsp70.

HSF1, the Transcription Factor That Regulates the Expression of Hsp27 and Hsp70, Decreases in C9-Treated MDA-MB-231 Cells. HSF1 is a transcription factor that induces the expression of genes with an upstream heat shock element, such as Hsp27 and Hsp70.[42] To further investigate the origin of the decrease in Hsp27 and Hsp70 levels as a consequence of C9 treatment, we compared the protein levels of heat shock factor 1 (HSF1) in MDA-MB-231 cells treated with either C9, 17-AAG or a combination of C9 and 17-AAG (Figure 6c).

We found that treatment of MDA-MB-231 cells with C9 alone or in combination with 17-AAG results in a substantial decrease of HSF1, while 17-AAG alone has a less drastic effect (Figure 6c). The decrease in the protein levels of HSF1 is most probably not a consequence of a change in its phosphorylation pattern because the WB does not show a slow migrating band (Supplementary Figure 5 in the Supporting Information). It is important to point out that WB assays coupled to SDS−PAGE do not necessarily inform about the oligomeric state of HSF1. In the absence of a thorough picture of how HSF1 is being affected by C9, our results nevertheless clearly show that 17-AAG has different effects on this transcription factor, and this is what is relevant in our data.

In conclusion, treatment of MDA-MB-231 cells with C9 alone or combined with 17-AAG induces a marked decrease in the protein levels of HSF1, an event that probably leads to the downregulation of Hsp27 and Hsp70. Clearly, the decrease of HSF1, like that of Cdc37 mentioned above, is an unexpected yet beneficial effect of C9.

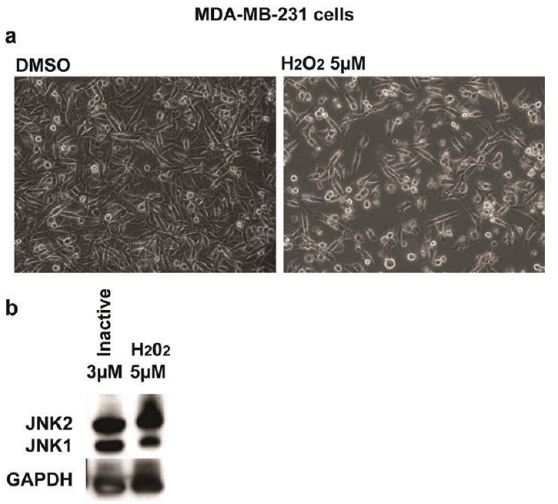

Figure 7. Killing and protein degradation effects of H_2O_2 on MDA-MB-231 cells. (a) MDA-MB-231 cell shape induction by H_2O_2 (5 μM), in a 24 h treatment. Pictures were taken at 20× magnification. (b) WB assays testing JNK1/2 in MDA-MB-231 cells treated 24 h with inactive compound (3 μM) or H_2O_2 (5 μM).

The Anticancer Effects of C9 Are Different from Those of a General Oxidizing Agent, H_2O_2. While preparing this manuscript we became aware that compounds with a pyrimidotriazole ring like C9 have been shown to cyclize *in vitro* and produce reactive oxygen species (ROS), when exposed to reducing agents.[43−45] To rule out such activity as the source of our observations, we compared the effects of C9 with those of a lethal dose of a strong ROS inducer, H_2O_2. Whereas treatment with C9 induces significant changes in cell shape (Figure 4a), the effects of treatment with H_2O_2 were very different: massive cell death and cell shrinkage (Figure 7a). We also tested by WB the protein levels of JNK1/2 (one of the unexpected C9 targets) and found that unlike C9 the level of this protein remained unchanged in cells treated with the inactive compound tested in Figure 2b or with H_2O_2 (Figure 7b).

These results show that two of the main unexpected effects of C9 in MDA-MB-231 cells observed here, which are the induction of cell shape change and the protein downregulation of JNK1/2, are not due to nonspecific induction of ROS.

DISCUSSION

The TNBC subtype represents about 10−20% overall of mammary tumors. TNBC cases are prevalent in young women mostly of African American origin.[46,47] Currently, the available target-specific drugs effective against breast cancer are inhibitors of the hormone receptors ER and PR and of the receptor tyrosine kinase HER2.[47] The TNBC subtype does not express any of these drug targets and is therefore particularly difficult to treat.[46,47]

It was originally thought that TNBC cells would not be sensitive to Hsp90 inhibitors, because they do not express classic targets such as HER2. Recent studies however have shown that the Hsp90 ATP-binding site inhibitors PU-H71 and NVP-AUY922 kill the drug-resistant TNBC cell line MDA-MB-231 in a 72 h treatment.[18,22] Like 17-AAG, an undesirable side effect

of PU-H71 and NVP-AUY922 treatment is that it induces an increase in the mRNA and protein levels of the antiapoptotic chaperone Hsp70.[18,22]

We have demonstrated that the novel chaperone inhibitor C9 is effective in killing breast cancer cell lines (BT-474 and MCF7), including the drug-resistant mammary TNBC subtype (MDA-231 and MDA-MB-468). Remarkably, treatment of MDA-MB-231 and MDA-MB-468 cells with C9 kills these TNBC cell lines in a 24 h exposure (Figure 2b and Supplementary Figure 1b in the Supporting Information), in contrast to the 72 h needed for PU-H71 and NVP-AUY922 to be lethal against MDA-MB-231 cells.[18,22]

Furthermore, C9 induces a change in cell shape, together with an inhibition of the characteristic migration properties characteristic of these cells, in a "scratch/wound-healing" assay (Figures 4a and 4b). An interesting feature of C9 is its ability to kill TNBC cell lines in a Caspase 3/7-independent manner (Figure 5a).

We also show that treating cells with C9 alone or combined with 17-AAG results in a decrease in the levels of a set of Hsp90-dependent client proteins (Cdk4, Raf-1, JNK1/2 and p38) (Figure 6a). The protein downregulation of these kinases in C9-treated cells is particularly interesting because in mammary cell lines the individual inactivation of JNK1/2 or p38 has been correlated with inhibition of cell migration.[48−50] Additionally, activated JNK1/2 is proapoptotic in a context-dependent manner[7] and has been shown to participate in the onset of apoptosis in breast cancer cell lines, under conditions of cellular stress.[51]

Our hypothesis is that the downregulation by C9 of the kinases p38 and JNK1/2, which are affected less drastically by 17-AAG, may explain at least in part the migration inhibition and Caspase 3/7-independent killing properties of C9. An alternative hypothesis is that the downregulation of Cdc37 is expected to have an effect on the total phosphorylation levels, which may in turn induce cytoskeletal rearrangements and thus account for the cell migration inhibition and change in cell shape induced by C9.

Finally, the decrease in the mRNA levels of Hsp27 and Hsp70 is most probably due to the drastic diminution in the protein levels of HSF1 induced by C9 (Figure 6c). Treating cells with a combination of C9 and either 17-AAG or NVP-AUY922 suppresses substantially the undesirable overexpression of Hsp70 (Figures 6c and 6d), which is a hallmark of these Hsp90 inhibitors. Another potential benefit of combining C9 with two of these compounds (17-AAG and NVP-AUY922) is that in a 24 h treatment the lethal-IC50 of C9 against MDA-MB-231 cells is slightly lower in comparison to that determined for C9 alone (Figure 2d).

Interestingly, C9 fails to counteract PU-H71's transcriptional upregulation of Hsp70, despite sharing a common binding site with the other HSP-90 inhibitors, 17-AAG or NVP-AUY922. Each of these Hsp90 inhibitors has a unique chemical structure, which in turn induces different allosteric conformational changes in the Hsp90 N-terminus.[1] The Hsp90 allosteric changes induced by PU-H71 are the most drastic, compared to 17-AAG or NVP-AUY922.[1] These differences are proposed to underpin the distinct anticancer properties of these Hsp90 inhibitors despite their common binding site in Hsp90[1] and may explain the inability of C9 to suppress PU-H71's transcriptional upregulation of HSP-70.

To summarize, our results suggest that C9 alone, or in combination with at least two Hsp90 ATP-binding site inhibitors currently in clinical trials (17-AAG and NVP-AUY922), could be an effective route to novel anticancer therapeutics, with a potential activity against the TNBC subtype. To define globally the effects and direct targets of C9 in cancer cells, future studies will include, respectively, a whole-cell quantitative profile of the transcript and protein levels; and a systematic investigation of the protein interactome associated with the Hsp70−HOP−Hsp90 chaperone complex.

■ ASSOCIATED CONTENT

Supporting Information. Five additonal figures as discussed in the text. This material is available free of charge via the Internet at http://pubs.acs.org.

■ AUTHOR INFORMATION

Corresponding Author

*Yale University, Department of Molecular Biophysics and Biochemistry, New Haven, CT, United States. E-mail: lynne.regan@yale.edu.

■ ACKNOWLEDGMENT

We are grateful to Ewa Menet at the Cell Sorting Facility, Yale University, who performed and analyzed the FACS experiments. Michael Salcius operated the plate reader at the Yale University Genomics and Proteomics Center. MDA-MB-231 cells were a kind gift of Dr. Anthony Koleske. This work was funded in part by grants from Joan's Legacy Lung Cancer Foundation and Mary Kay Ash (to L.R.). K.M.H. is an HHMI Fellow of the Damon Runyon Cancer Research Foundation.

■ REFERENCES

(1) Biamonte, M. A.; et al. Heat shock protein 90: inhibitors in clinical trials. *J. Med. Chem.* **2010**, *53* (1), 3–17.

(2) Janin, Y. L. ATPase inhibitors of heat-shock protein 90, second season. *Drug Discovery Today* **2010**, *15* (9−10), 342–53.

(3) Pearl, L. H.; Prodromou, C. Structure and mechanism of the Hsp90 molecular chaperone machinery. *Annu. Rev. Biochem.* **2006**, *75*, 271–94.

(4) Pratt, W. B.; Toft, D. O. Regulation of signaling protein function and trafficking by the hsp90/hsp70-based chaperone machinery. *Exp. Biol. Med. (Maywood)* **2003**, *228* (2), 111–33.

(5) Caplan, A. J.; Mandal, A. K.; Theodoraki, M. A. Molecular chaperones and protein kinase quality control. *Trends Cell Biol.* **2007**, *17* (2), 87–92.

(6) Powers, E. T.; et al. Biological and chemical approaches to diseases of proteostasis deficiency. *Annu. Rev. Biochem.* **2009**, *78*, 959–91.

(7) Powers, M. V.; Clarke, P. A.; Workman, P. Death by chaperone: HSP90, HSP70 or both? *Cell Cycle* **2009**, *8* (4), 518–26

(8) Kundrat, L.; Regan, L. Identification of residues on Hsp70 and Hsp90 ubiquitinated by the cochaperone CHIP. *J. Mol. Biol.* **2010**, *395* (3), 587–94.

(9) Kundrat, L. Regan, L.; , Balance between folding and degradation for Hsp90-dependent client proteins: a key role for CHIP. *Biochemistry*. *49*(35): p. 7428-38.

(10) Stebbins, C. E.; et al. Crystal structure of an Hsp90-geldanamycin complex: targeting of a protein chaperone by an antitumor agent. *Cell* **1997**, *89* (2), 239–50.

(11) Roe, S. M.; et al. Structural basis for inhibition of the Hsp90 molecular chaperone by the antitumor antibiotics radicicol and geldanamycin. *J. Med. Chem.* **1999**, *42* (2), 260–6.

(12) Solit, D. B.; et al. 17-Allylamino-17-demethoxygeldanamycin induces the degradation of androgen receptor and HER-2/neu and inhibits the growth of prostate cancer xenografts. *Clin. Cancer Res.* **2002**, *8* (5), 986–93.
(13) Ge, J.; et al. Design, synthesis, and biological evaluation of hydroquinone derivatives of 17-amino-17-demethoxygeldanamycin as potent, water-soluble inhibitors of Hsp90. *J. Med. Chem.* **2006**, *49* (15), 4606–15.
(14) Solit, D. B.; et al. Phase I trial of 17-allylamino-17-demethoxygeldanamycin in patients with advanced cancer. *Clin. Cancer Res.* **2007**, *13* (6), 1775–82.
(15) Solit, D. B.; et al. Phase II trial of 17-allylamino-17-demethoxygeldanamycin in patients with metastatic melanoma. *Clin. Cancer Res.* **2008**, *14* (24), 8302–7.
(16) McCollum, A. K.; et al. Up-regulation of heat shock protein 27 induces resistance to 17-allylamino-demethoxygeldanamycin through a glutathione-mediated mechanism. *Cancer Res.* **2006**, *66* (22), 10967–75.
(17) Maloney, A.; et al. Gene and protein expression profiling of human ovarian cancer cells treated with the heat shock protein 90 inhibitor 17-allylamino-17-demethoxygeldanamycin. *Cancer Res.* **2007**, *67* (7), 3239–53.
(18) Caldas-Lopes, E.; et al. Hsp90 inhibitor PU-H71, a multimodal inhibitor of malignancy, induces complete responses in triple-negative breast cancer models. *Proc. Natl. Acad. Sci. U.S.A.* **2009**, *106* (20), 8368–73.
(19) Gaspar, N.; et al. Mechanistic evaluation of the novel HSP90 inhibitor NVP-AUY922 in adult and pediatric glioblastoma. *Mol. Cancer Ther.* **2010**, *9* (5), 1219–33.
(20) Yi, F.; Regan, L. A novel class of small molecule inhibitors of Hsp90. *ACS Chem. Biol.* **2008**, *3* (10), 645–54.
(21) Hartl, F. U.; Hayer-Hartl, M. Converging concepts of protein folding in vitro and in vivo. *Nat. Struct. Mol. Biol.* **2009**, *16* (6), 574–81.
(22) Eccles, S. A.; et al. NVP-AUY922: a novel heat shock protein 90 inhibitor active against xenograft tumor growth, angiogenesis, and metastasis. *Cancer Res.* **2008**, *68* (8), 2850–60.
(23) Lu, Z.; Hunter, T. Degradation of activated protein kinases by ubiquitination. *Annu. Rev. Biochem.* **2009**, *78*, 435–75.
(24) Lopez-Otin, C.; Hunter, T. The regulatory crosstalk between kinases and proteases in cancer. *Nat. Rev. Cancer* **2010**, *10* (4), 278–92.
(25) Ota, A.; et al. Specific regulation of noncanonical p38alpha activation by Hsp90-Cdc37 chaperone complex in cardiomyocyte. *Circ. Res.* **2010**, *106* (8), 1404–12.
(26) Nieto-Miguel, T.; et al. Proapoptotic role of Hsp90 by its interaction with c-Jun N-terminal kinase in lipid rafts in edelfosine-mediated antileukemic therapy. *Oncogene* **2008**, *27* (12), 1779–87.
(27) Gutierrez, G. J.; et al. Interplay between Cdh1 and JNK activity during the cell cycle. *Nat. Cell Biol.* **2010**, *12* (7), 686–95.
(28) Yi, F.; et al. An AlphaScreen-based high-throughput screen to identify inhibitors of Hsp90-cochaperone interaction. *J. Biomol. Screening* **2009**, *14* (3), 273–81.
(29) Neve, R. M.; et al. A collection of breast cancer cell lines for the study of functionally distinct cancer subtypes. *Cancer Cell* **2006**, *10* (6), 515–27.
(30) Munster, P. N.; et al. Inhibition of heat shock protein 90 function by ansamycins causes the morphological and functional differentiation of breast cancer cells. *Cancer Res.* **2001**, *61* (7), 2945–52.
(31) Pickl, M.; Ries, C. H. Comparison of 3D and 2D tumor models reveals enhanced HER2 activation in 3D associated with an increased response to trastuzumab. *Oncogene* **2009**, *28* (3), 461–8.
(32) Weigelt, B.; Lo, A. T.; Park, C. C.; Gray, J. W.; Bissell, M. J. HER2 signaling pathway activation and response of breast cancer cells to HER2-targeting agents is dependent strongly on the 3D microenvironment. *Breast Cancer Res. Treat.* **2010**, *122* (1), 35–43.
(33) Ivascu, A.; Kubbies, M. Diversity of cell-mediated adhesions in breast cancer spheroids. *Int. J. Oncol.* **2007**, *31* (6), 1403–13.
(34) Korkaya, H.; et al. HER2 regulates the mammary stem/progenitor cell population driving tumorigenesis and invasion. *Oncogene* **2008**, *27* (47), 6120–30.
(35) Wolf, K.; et al. Compensation mechanism in tumor cell migration: mesenchymal-amoeboid transition after blocking of pericellular proteolysis. *J. Cell Biol.* **2003**, *160* (2), 267–77.
(36) Xu, W.; et al. Sensitivity of mature Erbb2 to geldanamycin is conferred by its kinase domain and is mediated by the chaperone protein Hsp90. *J. Biol. Chem.* **2001**, *276* (5), 3702–8.
(37) Theodoraki, M. A.; et al. Akt shows variable sensitivity to an Hsp90 inhibitor depending on cell context. *Exp. Cell Res.* **2007**, *313* (18), 3851–8.
(38) Smith, J. R.; et al. Silencing the cochaperone CDC37 destabilizes kinase clients and sensitizes cancer cells to HSP90 inhibitors. *Oncogene* **2009**, *28* (2), 157–69.
(39) Zhang, T.; et al. A novel Hsp90 inhibitor to disrupt Hsp90/Cdc37 complex against pancreatic cancer cells. *Mol. Cancer Ther.* **2008**, *7* (1), 162–70.
(40) Ota, A.; et al. Specific regulation of noncanonical p38alpha activation by Hsp90-Cdc37 chaperone complex in cardiomyocyte. *Circ. Res.* **2010**, *106* (8), 1404–12.
(41) Garrido, C.; et al. Heat shock proteins 27 and 70: anti-apoptotic proteins with tumorigenic properties. *Cell Cycle* **2006**, *5* (22), 2592–601.
(42) Voellmy, R. On mechanisms that control heat shock transcription factor activity in metazoan cells. *Cell Stress Chaperones* **2004**, *9* (2), 122–33.
(43) Johnston, P. A.; et al. Development of a 384-well colorimetric assay to quantify hydrogen peroxide generated by the redox cycling of compounds in the presence of reducing agents. *Assay Drug Dev. Technol.* **2008**, *6* (4), 505–18.
(44) Johnston, P. A. Redox cycling compounds generate H_2O_2 in HTS buffers containing strong reducing reagents—real hits or promiscuous artifacts? *Curr Opin. Chem. Biol.* **2011**, *15* (1), 174–82.
(45) Soares, K. M.; et al. Profiling the NIH Small Molecule Repository for compounds that generate H2O2 by redox cycling in reducing environments. *Assay Drug Dev. Technol.* **2010**, *8* (2), 152–74.
(46) Stockmans, G.; et al. Triple-negative breast cancer. *Curr. Opin. Oncol.* **2008**, *20* (6), 614–20.
(47) Carey, L.; et al. Triple-negative breast cancer: disease entity or title of convenience? *Nat Rev. Clin. Oncol.* **2010**, *7* (12), 683–92.
(48) Huang, C.; et al. JNK phosphorylates paxillin and regulates cell migration. *Nature* **2003**, *424* (6945), 219–23.
(49) Shin, I.; et al. H-Ras-specific activation of Rac-MKK3/6-p38 pathway: its critical role in invasion and migration of breast epithelial cells. *J. Biol. Chem.* **2005**, *280* (15), 14675–83.
(50) Kaoud, T. S.; et al. Development of JNK2-Selective Peptide Inhibitors That Inhibit Breast Cancer Cell Migration. *ACS Chem. Biol.* **2011**, *6* (6), 658–66.
(51) Mingo-Sion, A. M.; et al. Inhibition of JNK reduces G2/M transit independent of p53, leading to endoreduplication, decreased proliferation, and apoptosis in breast cancer cells. *Oncogene* **2004**, *23* (2), 596–604.